A multi-frequency radio continuum study of the edge-on galaxy NGC 3556

Bruyn, A.G. de; Hummel, E.

Astron. Astrophys. 73, 196–201 (1979)

ASTRONOMY AND ASTROPHYSICS

A Multi-frequency Radio Continuum Study of the Edge-on Galaxy NGC 3556

A. G. de Bruyn[1] and E. Hummel[2]

[1] Sterrewacht Leiden, The Netherlands, and Hale Observatories, Carnegie Institution of Washington, California Institute of Technology, Pasadena, Calif., USA

[2] Kapteyn Astronomical Institute, P. O. Box 800, 9700 AV Groningen, The Netherlands

Received June 30, 1978

Summary. We observed the radio continuum radiation of the edge-on galaxy NGC 3556 at wavelengths of 49, 21, and 6 cm. The 21 cm observations show the existence of an extended, weak halo component with dimensions of about 10 kpc in the direction perpendicular to the plane of the galaxy. The spectral index distribution, derived from the 49 and 21 cm maps, indicates a steepening of the radiospectrum when going to the edge of the galaxy. Some suggestions for the interpretation of this steepening are given. The 6 cm observations only give information on the central source, which, at the resolution of $6''.9 \times 8''.3$, breaks up in a number of discrete sources.

Key words: spiral galaxy – radio continuum emission – halo – cosmic rays

1. Introduction

NGC 3556 is a late-type galaxy (Hubble-Sandage type Sc) seen close to edge-on. High resolution radio continuum observations at 1415 MHz (van der Kruit, 1973a, b) showed that NGC 3556 possesses a thick disk of intermediate brightness and possibly some faint extensions out of the plane. We have undertaken an extensive radio continuum study of this galaxy because of the importance of radio continuum haloes around spiral galaxies in relation to the confinement, dynamics and lifetime of cosmic ray particles (e.g. Ginzburg, 1974; Ginzburg and Ptuskin, 1976). Although the inclination of the equatorial plane of NGC 3556 is not ideal for a study of the halo, there are only a few other galaxies with a more favourable inclination that also have a high radio surface brightness and large angular extent.

The late morphological type and somewhat chaotic optical appearance of NGC 3556 (e.g. de Vaucouleurs, 1958) make it difficult to determine an accurate value of its inclination. De Vaucouleurs (1958) who classifies the galaxy as a late-type barred spiral, finds $i=82°$, and Burbidge et al. (1960) give $i=84°$ determined from the curvature of the dust lane. On the other hand, the optical axis ratios at isophotes of $26^m.5/\square''$ (Holmberg, 1958) and $25^m/\square''$ (de Vaucouleurs et al., 1976) are 2.5 and 3.3, respectively. Because of the uncertainty in the optically determined inclination we will adopt an inclination of 74° as derived from H I observations with the Westerbork Synthesis Radio Telescope (Shostak, private communication).

No central bulge or nucleus is visible. Furthermore, we note that the galaxy is rich in neutral hydrogen (Roberts, 1968; Rogstad et al., 1967) and has a rather low rotation velocity with peak values of 100–150 km s^{-1} (Burbidge et al., 1960; Rogstad et al., 1967). In the following we adopt a distance of 15 Mpc, as derived from the radial velocity and assuming a Hubble constant of 50 km s^{-1} Mpc^{-1}. At this distance, 1′ corresponds to 4.36 kpc.

Send offprint requests to: E. Hummel

2. Observations and Reduction

Radio continuum observations were carried out with the Westerbork Synthesis Radio Telescope (WSRT) at frequencies of 610, 1410, and 4995 MHz (wavelengths of 49, 21, and 6 cm, respectively). For a description of the telescope, its principles of operation, calibration and reduction procedures we refer to Högbom and Brouw (1974), Casse and Muller (1974), and van Someren Gréve (1974).

The present 1410 MHz data has nearly twice the sensitivity as the earlier observations at 1415 MHz by van der Kruit (1973a). We observed at a slightly lower frequency to avoid contamination by 21 cm line emission from the western part of the galaxy (cf. Sect. 3.1). Table 1 gives a summary of the observations and instrumental characteristics at the three available wavelengths.

In addition to the full resolution maps (cf. Table 1) we have also constructed lower resolution maps at 6 and 21 cm to compare with the full resolution 21 and 49 cm maps, respectively. Before comparison the individual maps were cleaned (Högbom, 1974) in order to get identical gaussian beams. This can be done unambiguously because the U, V plane was sufficiently sampled. The maps were corrected for small residual zero-level offsets, which are due to the missing zero spacing.

Since our shortest baseline and baseline increment are 36 m at all three wavelengths, we fully sampled emission on angular scales $\leqq 47'$ (49 cm), $\leqq 20'$ (21 cm), and $\leqq 5'.7$ (6 cm), respectively (cf. Bracewell, 1958). Since the 49-cm map gives no indication of structure larger than about 8′, the cleaned 49 and 21-cm maps do not miss any flux. At 6 cm, however, this is not the case and the spectral index comparison between 6 and 21 cm is limited to a relatively bright central emission feature, taking proper account of the different sensitivities at 6 and 21 cm to extended disk emission.

3. Results

3.1. 21 cm Data

Figure 1 shows the 21 cm full resolution map superimposed on a print reproduced from a IIIa-J plate taken by Dr. H. C. Arp with the Palomar 48-inch Schmidt telescope. Our map agrees well with

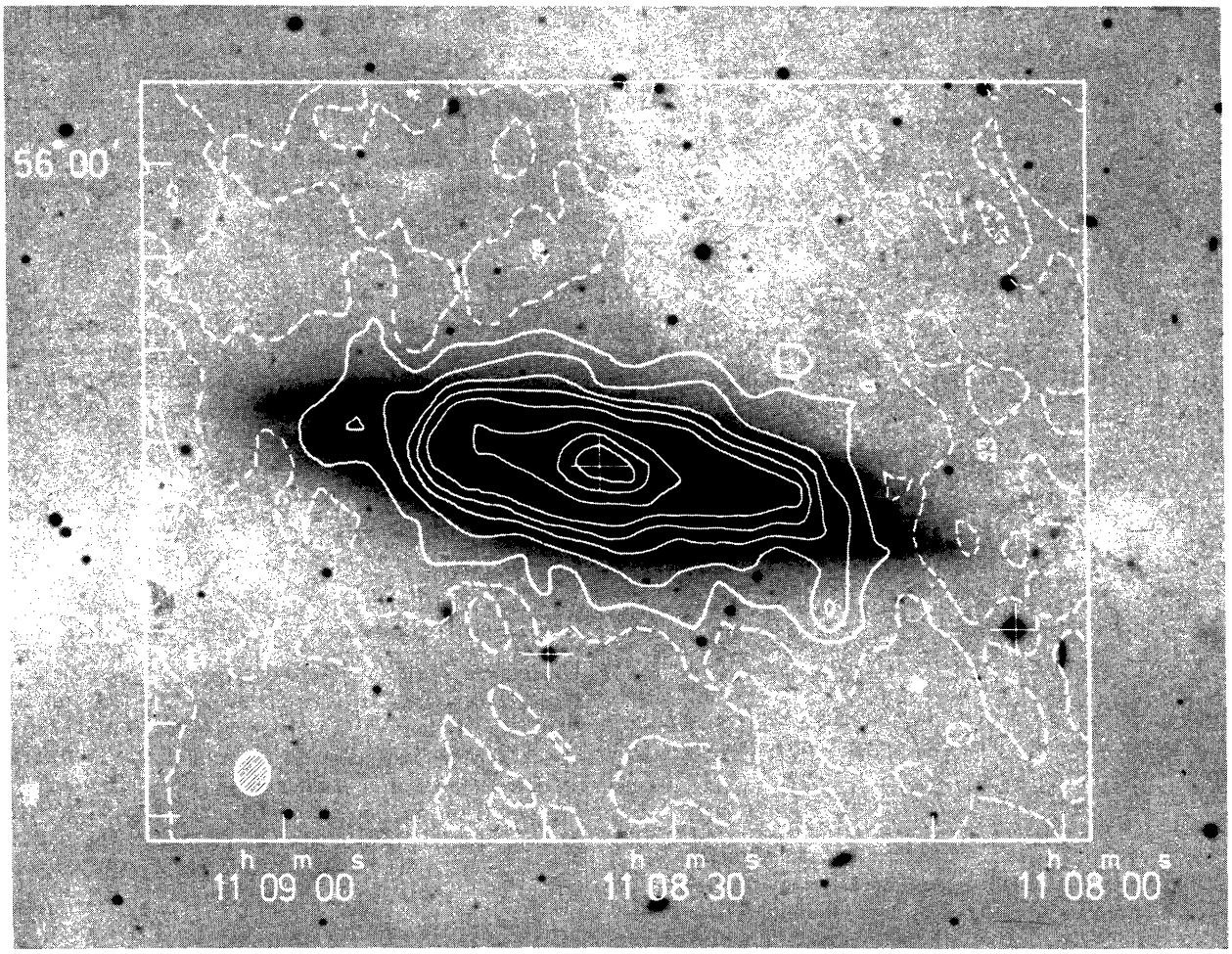

Fig. 1. The full resolution 21 cm continuum map superimposed on a deep IIIa-J photograph. The beam is indicated by the shaded ellipse. Contour values are −1.0, 0, 1.0, 2.0, 3.0, 4.0, 5.0, 10.0, 15.0, 20.0 mJy per beam. The r.m.s. noise is 0.4 mJy per beam. The optical center is indicated by a cross

Table 1. Observations and instrumental parameters

Frequency/ Wavelength	MHz cm	4995 6.0	1410 21.3	610 49.2
Observing dates		9 April 1974 13 May 1974	1 July 1975 28 July 1975	28 January 1975 30 January 1975
Field center (1950.0)		$11^h08^m36^s$ $+55^o57'00''$	$11^h08^m40^s$ $+55^o55'48''$	$11^h08^m53^s$ $+56^o00'00''$
Total observing time	hours	2 × 12	2 × 12	2 × 12
Baseline coverage[a]	meters	36 (36) 1440	36 (36) 1440	36 (36) 1440
Synthesized beam (RA × Dec)	arc s	6.9 × 8.3	24 × 29	56 × 68
Flux density to brightness temperature conversion	K/mJy	1.0	1.0	1.0
Grating ring separation (RA × Dec)	arc min	5.7 × 6.9	20.3 × 24.5	47 × 57

a To read as: shortest baseline (increment) longest baseline

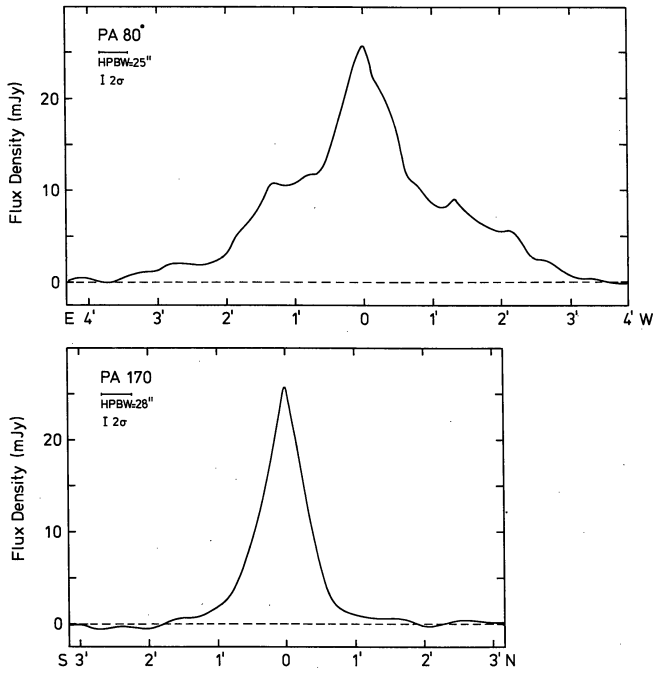

Fig. 2. Intensity profiles at 21 cm along the major axis (p.a. = 80°) and the minor axis (p.a. = 170°). The profiles are centered at the optical centroid

that of van der Kruit (1973a) except on the western side of the galaxy where the emission cuts off earlier and also is somewhat fainter. This difference can be ascribed to contaminating 21 cm line emission in van der Kruit's map (the line emission lies near one of the half-power points of the 4 MHz system bandpass).

As indicated by the superposition in Fig. 1, the emission along the galaxy minor axis reaches beyond the easily visible part of the optical disk, in contrast to the situation along the major axis. This is reflected in the fact that the radio axial ratio of 2.2 (small correction for beam smearing have been applied), is much less that the optical axial ratio of about 3.5 as determined from this photograph. The latter is in good agreement with the value given by de Vaucouleurs et al. (1976) which refers to a somewhat fainter isophote.

Fig. 2 shows intensity profiles along the major axis (p.a. = 80°), and minor axis (p.a. = 170°). The profile along the major axis shows a disk component and an extended central region with a brightness of about 13 mJy/beam area[1], and a half power width of 40″. In the profile along the minor axis it is not possible to separate the central region from the disk component. However, a faint component can be seen which has a surface brightness 10–20% of that of the inner region. At the 2.5σ level this component covers an approximately rectangular area of dimensions 6′.0 × 2′.7, (corrected for beam smearing).

The flux density of the galaxy, integrated over an area of 9′ × 5′, at 21 cm is 293 ± 15 mJy.

3.2. 6 cm *Data*

The full resolution 6 cm map is shown in Fig. 3 superimposed on a copy of the photograph illustrated in the Hubble Atlas. Only the small central region is bright enough to stand out above the noise. It is seen to break up into many discrete blobs and some elongated features parallel to the galaxy major axis. The northernmost blob coincides with an H II region. The remaining components are of too low surface brightness to show up at this resolution. At 6 cm not all the emission from the galaxy could be recovered in the clean procedure and no integrated flux density at 6 cm could therefore be determined.

3.3. 49 cm *Data*

The 49 cm map is shown in Fig. 4. The larger synthezised beam has blended the components seen in the higher resolution maps. In fact, the only evidence for a thick disk at 49 cm lies in the larger major-to-minor axis ratio in the radio compared to that in the optical regime.

The flux density, integrated over an area of 11′ × 6′, at 49 cm is 575 ± 25 mJy.

4. The Radio Spectrum

4.1. *The Integrated Spectrum*

The radio spectrum of the integrated emission is shown in Fig. 5. The 5000 MHz measurement is probably 10–20% too low because NGC 3556 is partially resolved with the NRAO 300-ft antenna at 5000 MHz. Our value for the total flux at 1410 MHz is somewhat less than that of van der Kruit (1973a, b) because of the problem of 21 cm line contamination referred to earlier. The radio spectrum can be fitted by a single power law with index[2] $\alpha = -0.85 \pm 0.05$ over the frequency range from 610 MHz to 4995 MHz.

4.2. *The Spectral Index Map*

With the clean and convolution procedure described in Sect. 2 we have constructed maps of the radio continuum radiation at 21 and 49 cm which have identical beam shape with an HPBW of 56″ × 68″. The spectral index map derived from them is shown in Fig. 6. The boundary of the spectral index map is the 5 mJy/beam area contour of the convolved 21 cm map.

The r.m.s. noise in the 56″ × 68″ 21 and 49 cm maps is 0.8 and 1.5 mJy/beam area, respectively. Since the zero level of both maps is well determined, noise is the main source of uncertainty in the spectral index map. The 1σ errors in the 21 and 50 cm maps cause an error in the spectral index which varies from 0.02 in the central region to 0.2 at the edges.

The region with the flattest spectral index $\alpha > -0.3$ lies in the southwestern part of the galaxy. It is interesting to note that at that position the emission shows a discrete peak (cf. Fig. 1). We suspect this peak to be due to a background source with a flat spectrum. If we ignore that region, it is clear that in general the spectrum steepens toward the edge of the galaxy. In the central region we see a relatively flat spectrum ($-0.6 < \alpha < -0.4$) and at the edge of the galaxy the spectral index decreases to values less than -1.0.

Comparison of the 6 cm map, smoothed to a 24″ × 29″ resolution, with the 21 cm full resolution map indicates that the central region, corrected for the disk contribution, has a much flatter spectral index of about -0.25.

1 1 mJy = 10^{-29} W Hz^{-1} m^{-2}

2 Spectral index defined as $S \propto \nu^{\alpha}$

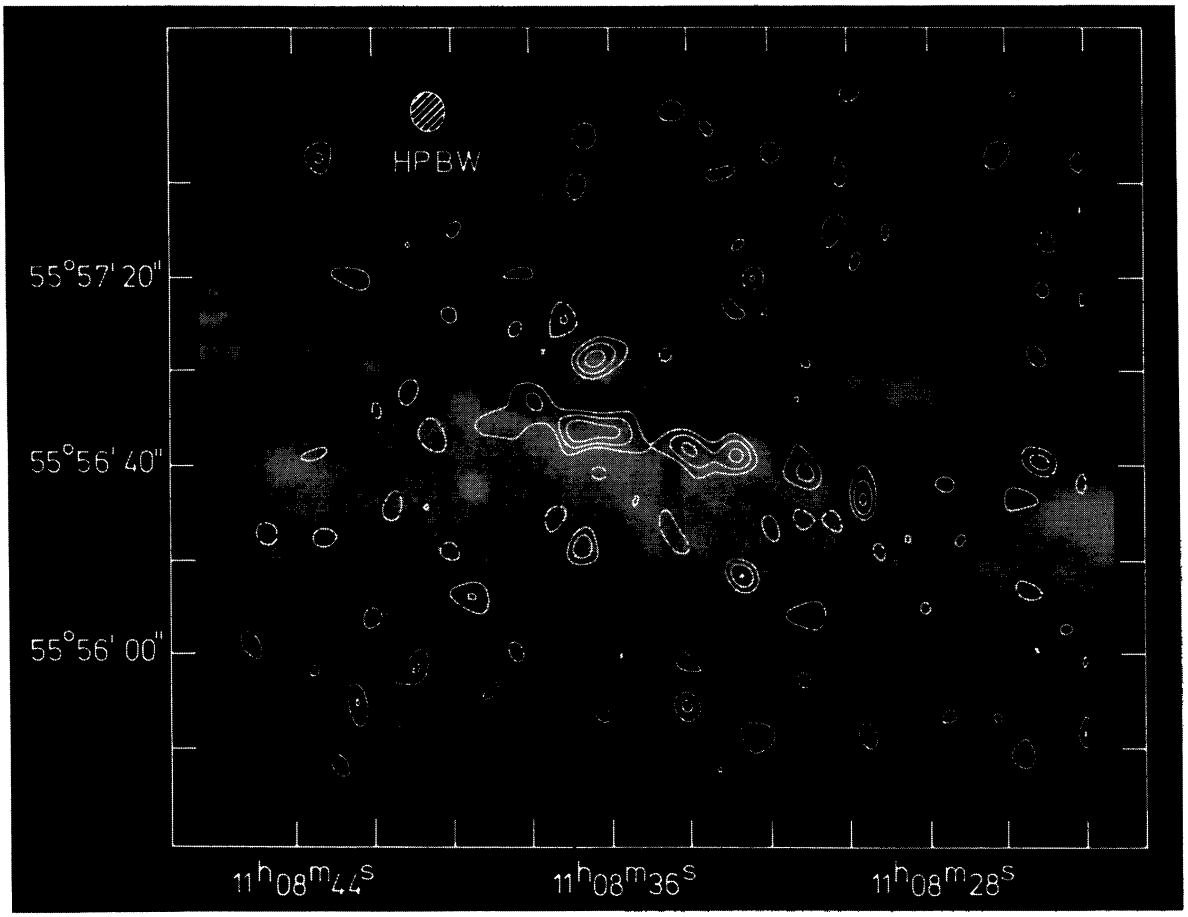

Fig. 3. Contours of the 6 cm radio emission of the central region of NGC 3556 superimposed on an optical photograph (courtesy Hale Observatories). Contour values are −2.25, −1.5, 1.5, 2.25, 3.0 mJy per beam. The r.m.s. noise is 0.75 mJy per beam

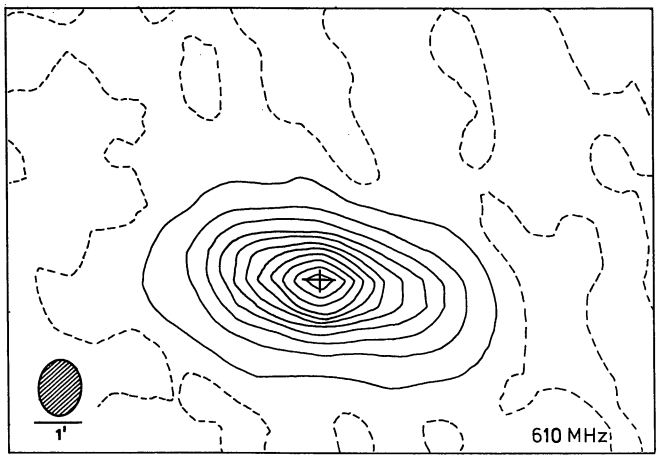

Fig. 4. The 49 cm continuum map. Contour values are 0, 5, and then in steps of 10 mJy up to 105 mJy per beam. The r.m.s. noise is 1.5 mJy per beam

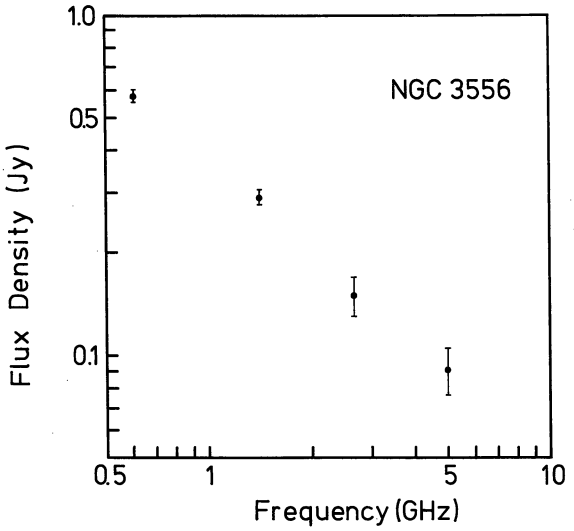

Fig. 5. The radio spectrum of the integrated emission of NGC 3556. The data at 610 and 1410 MHz are from this paper, while the data at 2695 and 5000 MHz are from de Jong (1967) and Sramek (1975), respectively

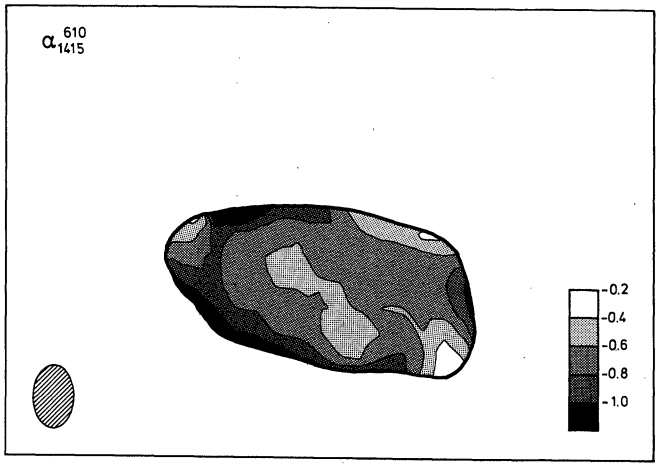

Fig. 6. Contour map of the spectral index distribution between 21 and 49 cm. The boundary of the spectral index map is the 5 mJy per beam contour of the 56″ × 68″ 21 cm map. The beam is indicated and has a halfwidth of 56″ × 68″

5. Discussion

The non-thermal radio spectrum of NGC 3556 shows that the radiation is largely due to synchrotron emission from relativistic electrons in a magnetic field. Although the brightness and spectral index distribution of the non-thermal emission yield some information on the sources and confinement region of the relativistic electrons, there is still much freedom in choosing the model appropriate to NGC 3556. In the following, we will therefore limit ourselves to a brief discussion of the most interesting properties of NGC 3556.

5.1. The Halo Component

The small axial ratio of the lowest contour in the full resolution 21 cm map, compared with the optical axial ratio, indicates a rather large z-extent of the radio continuum emission (the z-coordinate is perpendicular to the plane).

At a 2σ level the total width in the z-direction is about 3′ and the beam corrected width becomes 2′.7. This results in a linear scale for the projected z-thickness of about 12 kpc. If we model this low brightness component, the halo, as an oblate spheroid with an uniform volume emissivity seen under an inclination of 74°, the true z-thickness near the center of the galaxy must be 9–10 kpc, and the halo brightness per unit depth at 21 cm is about 0.1–0.2 K/kpc. The halo is estimated to contribute about 25% of the total emission of NGC 3556 at 21 cm.

The emissivity in the halo and disk cannot be fitted exactly with a single exponential function along the z-coordinate. A similar conclusion was reached by Allen et al. (1978) for the case of NGC 891. Unfortunately, the inclination of NGC 3556 is not high enough to determine accurately the thickness of the radio disk from our observations. Assuming a thickness to half-power of 0.75 kpc [similar to the value for NGC 891 (Allen et al., 1978) and our own galaxy (Baldwin, 1967)], we find that the volume emissivity in the halo at 21 cm is, on average, about 3% of that in the disk outside the central region. The uncertainty in this figure is, however, at least a factor two.

5.2. The Spectral Index Variation

The rather flat spectral index between 6 and 21 cm of the central region, encompassing the features seen in Fig. 3, suggests that most of its emission might be of thermal origin. This central complex contributes about 20% of the 21 cm flux density at that position. Removing this contribution leads to an approximately constant spectral index of -0.7 ± 0.05 over an area of about 4′ (=17 kpc) along the major axis. Beyond a radius of 2′ and at considerable z-distances the spectrum steepens considerably and we think it unlikely that this steepening is an artifact of an abrupt change in the level of thermal contamination [in the way envisaged by van der Kruit et al. (1977) for NGC 6946]. If, for example, the -0.7 spectral index were the result of a combination of a non-thermal component with $\alpha \leqq -0.9$ and a thermal component with $\alpha = -0.1$, the required amount of thermal emission at 21 cm would be about 30% of the total 21 cm flux density. At 6 cm this results in a total flux density of 140 mJy and here a conflict arises with the 6 cm flux density of 90 ± 13 mJy as measured by Sramek (1975). The spectral steepening towards the outer parts and into the halo must therefore be interpreted within the framework of synchrotron theory, and the following hypotheses will be considered. i) The electron injection spectrum steepens in the outer parts, ii) The injection spectrum is curved (convex) and the magnetic field strength is lower in the outer parts, iii) Ageing effects of the relativistic electrons are important.

Option i) seems ad hoc and also requires a source of particles in the halo which we consider unlikely. Option ii) implies a change of the index γ of the electron injection spectrum from $\gamma=2.4$ to $\gamma>3$ at an energy of about 5–10 GeV assuming an equipartition field strength of $5\ 10^{-6}$ Gauss in the disk and at least a factor four less than this in the outer disk and halo. Although this hypothesis cannot be excluded, we prefer the third alternative mainly because the very presence of relativistic electrons at up to 5 kpc above the plane suggests, for conventional propagation models, that these particles must be 10^{7-8} yr old. On this time scale inverse Compton and synchrotron losses become important. Segalovitz (1976) has shown that with a source function of very small size the spectral steepening already occurs close to the injection region. If the sources are confined to the optical disk the source function in the z-direction is small and changes in spectral index of 0.1 are achieved within 0′.5. At large radial distances from the center, where the source function probably decreases, the same effect can occur. Because the spectral index changes in the z-direction occur on a smaller linear scale than in the radial direction, diffusion in the z-direction is probably a more efficient mechanism of particle depletion in the disk than radial diffusion plus radiation losses.

Acknowledgements. We thank Dr H. C. Arp for a print copy of his plate of NGC 3556, and Drs Ekers and Sancisi for comments on the manuscript. This paper was written while one of us (A. G. de B.) held a Carnegie Fellowship at the Hale Observatories. We are grateful to Dr Babcock and the Carnegie Institution of Washington for these privileges. E. Hummel acknowledges financial support from the Netherlands Organization for Advancement of Pure Research (Z.W.O.). The Westerbork Synthesis Radio Telescope is operated by the Netherlands Foundation for Radio Astronomy with financial support from Z.W.O.

References

Allen, R. J., Baldwin, J. E., Sancisi, R.: 1978, *Astron. Astrophys.* **62**, 397

Baldwin, J. E.: 1967, in *Radio Astronomy and the Galactic System*, I.A.U. *Symposium* **31**, p. 337. Ed. H. van Woerden

Bracewell, R. N.: 1958, *Proc. IRE* **46**, 97

Burbidge, E. M., Burbidge, G. R., Prendergast, K. H.: 1960, *Astrophys. J.* **131**, 549

Casse, J. L., Muller, C. A.: 1974, *Astron. Astrophys.* **31**, 333

de Vaucouleurs, G.: 1958, *Astrophys. J.* **127**, 487

de Vaucouleurs, G., de Vaucouleurs, A., Corwin, H. G.: 1976, Second Reference Catalogue of Bright Galaxies, Austin: University of Texas Press

Ginzburg, V. L.: 1974, *Philos. Trans. Roy. Soc. London, A* **277**, 463

Ginzburg, V. L., Ptuskin, V. S.: 1976, *Rev. Mod. Phys.* **48**, 161

Högbom, J. A.: 1974, *Astron. Astrophys. Suppl.* **15**, 417

Högbom, J. A., Brouw, W. N.: 1974, *Astron. Astrophys.* **33**, 289

Holmberg, E.: 1958, *Medd. Lund. Obs. II*, No. 136

Jong, M. L. de: 1967, *Astrophys. J.* **150**, 1

Kruit, P. C. van der: 1973a, *Astron. Astrophys.* **29**, 249

Kruit, P. C. van der: 1973b, *Astron. Astrophys.* **29**, 263

Kruit, P. C. van der, Allen, R. J., Rots, A. H.: 1977, *Astron. Astrophys.* **55**, 421

Roberts, M. S.: 1968, *Astron. J.* **73**, 945

Rogstad, D. H., Rougoor, G. W., Whiteoak, J. B.: 1967, *Astron. J.* **150**, 9

Segalovitz, A.: 1976, Ph. D. Thesis, Sterrewacht Leiden

Someren Gréve, H. W. van: 1974, *Astron. Astrophys.* **15**, 343

Sramek, R. A.: 1975, *Astron. J.* **80**, 771